



CHORUS

This is the accepted manuscript made available via CHORUS. The article has been published as:

Coupling between dynamic magnetic and charge-order correlations in the cuprate superconductor

$\text{Nd}_{2-x}\text{Ce}_x\text{CuO}_4$

E. H. da Silva Neto, M. Minola, B. Yu, W. Tabis, M. Bluschke, D. Unruh, H. Suzuki, Y. Li, G. Yu, D. Betto, K. Kummer, F. Yakhou, N. B. Brookes, M. Le Tacon, M. Greven, B. Keimer, and A. Damascelli

Phys. Rev. B **98**, 161114 — Published 17 October 2018

DOI: [10.1103/PhysRevB.98.161114](https://doi.org/10.1103/PhysRevB.98.161114)

Coupling between dynamic magnetic and charge-order correlations in the cuprate superconductor $\text{Nd}_{2-x}\text{Ce}_x\text{CuO}_4$

E. H. da Silva Neto,^{1,2,3,*} M. Minola,³ B. Yu,⁴ W. Tabis,^{5,6,7} M. Bluschke,^{3,8}
D. Unruh,¹ H. Suzuki,³ Y. Li,⁴ G. Yu,⁴ D. Betto,⁹ K. Kummer,⁹ F. Yakhou,⁹
N. B. Brookes,⁹ M. Le Tacon,^{3,10} M. Greven,⁴ B. Keimer,³ and A. Damascelli^{2,11,†}

¹*Department of Physics, University of California, Davis, California 95616, USA*

²*Quantum Matter Institute, University of British Columbia, Vancouver, British Columbia V6T 1Z4, Canada*

³*Max Planck Institute for Solid State Research, Heisenbergstrasse 1, D-70569 Stuttgart, Germany*

⁴*School of Physics and Astronomy, University of Minnesota, Minneapolis, Minnesota 55455, USA*

⁵*Laboratoire National des Champs Magnétiques Intenses, CNRS UPR-3228, 31400, Toulouse, France*

⁶*AGH University of Science and Technology, Faculty of Physics and Applied Computer Science, 30-059 Krakow, Poland*

⁷*Institute of Solid State Physics, TU Wien, 1040 Vienna, Austria*

⁸*Helmholtz-Zentrum Berlin für Materialien und Energie, BESSY II, Albert-Einstein-Str. 15, 12489 Berlin, Germany*

⁹*European Synchrotron Radiation Facility, 71 Avenue de Martyrs, CS40220, F-38043 Grenoble Cedex 9, France*

¹⁰*Institut für Festkörperphysik, Karlsruher Institut für Technologie, 76201 Karlsruhe, Germany*

¹¹*Department of Physics & Astronomy, University of British Columbia, Vancouver British Columbia, V6T 1Z1, Canada*

Charge order has now been observed in several cuprate high-temperature superconductors. We report a resonant inelastic x-ray scattering experiment on the electron-doped cuprate $\text{Nd}_{2-x}\text{Ce}_x\text{CuO}_4$ that demonstrates the existence of dynamic correlations at the charge order wave vector. Upon cooling we observe a softening in the electronic response, which has been predicted to occur for a d -wave charge order in electron-doped cuprates. At low temperatures, the energy range of these excitations coincides with that of the dispersive magnetic modes known as paramagnons. Furthermore, measurements where the polarization of the scattered photon is resolved indicate that the dynamic response at the charge order wave vector primarily involves spin-flip excitations. Overall, our findings indicate a coupling between dynamic magnetic and charge-order correlations in the cuprates.

In addition to the long-studied superconducting (SC), antiferromagnetic (AF), and pseudogap phases, the copper-based high-temperature superconductors (cuprates) also feature charge order (CO) correlations. The CO is a periodic organization of low-energy electronic states and it is ubiquitous to all cuprate families¹⁻¹⁶. Early theoretical works that predicted an instability toward an intertwined pattern of charge and spin order, known as stripes¹⁷⁻²⁰, were first confirmed by neutron scattering experiments in the La-based family, *i.e.* $(\text{La,Nd})_{2-x}(\text{Ba,Sr})_x\text{CuO}_4$ ¹. In more recent years, the observation of CO in other cuprate families has led to new theories that suggest a tight link between the emergence of CO and AF fluctuations²¹⁻²⁵. However, the possibility of such an interplay in non-stripe materials remains controversial. Several studies show no clear correlation between the doping evolution of the CO with that of the AF properties^{14,26,27}, except for the case of Zn-doped $\text{YBa}_2\text{Cu}_3\text{O}_{6+\delta}$ (YBCO), where magnetic order is nucleated by Zn impurities at the expense of the CO²⁸. Nuclear magnetic resonance experiments in YBCO also suggest the possibility that charge and spin fluctuations might be coupled^{5,27,29}. Still, a clear connection between CO and AF correlations remains elusive due to the lack of experiments that simultaneously resolve the excitations of both charge and spin degrees of freedom. The electron-doped cuprate $\text{Nd}_{2-x}\text{Ce}_x\text{CuO}_4$ (NCCO), featuring more prominent AF correlations than its hole-doped counterparts³⁰, also develops CO¹³, making it an ideal system where to investigate the relation between AF and

CO correlations.

Although static CO has been detected by a variety of experiments that probe electrons at long time scales, momentum-resolved evidence for dynamic CO correlations has proven to be more elusive. In YBCO, where the CO is the strongest (apart from the special case of stripes in La-cuprates), Cu- L_3 resonant inelastic x-ray scattering (RIXS) shows that the CO is quasi-elastic within 130 meV⁶, and non-resonant inelastic X-ray scattering indicates that the lattice distortion associated with the CO is static within 1.4 meV³¹. However, several experiments^{5,29,32-34} showed that the intensity and correlation length of the CO, in a narrow doping range of YBCO, are dramatically enhanced in magnetic fields above 12 T, suggesting that the short-range (≈ 65 Å) CO at zero field is likely a precursor state to the high field CO. Even shorter-range CO correlations (≈ 25 Å) are observed in most other cuprates, including electron-doped materials^{9,10,12-14,16}. Thus, it is possible that the zero-field CO correlations in the cuprates are primarily dynamic in nature³⁵⁻³⁷ and their observation by static probes is the result of disorder pinning. More recently, a RIXS study reported the observation of CO excitations at low-energies (≈ 60 meV) in $\text{Bi}_2\text{Sr}_2\text{CaCu}_2\text{O}_{8+\delta}$ ³⁸, although a coupling to magnetic correlations was not reported.

Over the last few years, Cu- L_3 resonant X-ray scattering, either in energy-integrated mode (EI-RXS) or in energy-resolved inelastic mode (RIXS), has become the tool of choice for the detection of CO in the cuprates.

In both cases, tuning of the photon energy to the Cu- L_3 edge enhances the sensitivity of the scattering cross-section to the low-energy electronic states that derive from the CuO_2 planes. In a typical EI-RXS measurement, all photons scattered into a reciprocal-lattice element are picked up by the detector, whereas in RIXS the scattered photons are analyzed by a spectrometer that resolves their energy. Consequently, the EI-RXS measurements (e.g. ^{9,10,13,26,39}) cannot rule out the contribution of inelastic scattering to the broad CO peaks in momentum space. Here, we exploit the high-resolution ERIXS spectrometer at the ID32 beamline at the European Synchrotron Radiation Facility to uncover the presence of dynamic correlations at the charge order wave vector in the (Q_{CO} , in-plane momentum) in both non-SC ($x = 0.106$) and SC ($x = 0.145$) NCCO. We used the same samples studied in prior EI-RXS work¹⁴, which were obtained from larger crystals for which antiferromagnetic correlations were previously measured^{30,40,41}. We find that a large contribution to the dynamic correlations at Q_{CO} occurs in the same energy range spanned by the magnetic excitations. By resolving the polarization of the scattered photons, we find that this enhancement of the dynamic response at Q_{CO} is mostly due to spin-flip processes, thus showing a direct coupling between dynamic magnetic and charge-order correlations in NCCO.

Figure 1(a) shows select Cu- L_3 RIXS spectra measured at different values of H , the in-plane momentum transfer in reciprocal lattice units (rlu), with an energy resolution of approximately 60 meV (full width at half maximum)⁴¹. This information can be compiled in a single color plot, Fig.1(b), which shows the energy-momentum structure of excitations in NCCO, including the elastic line ($E = 0$ eV) and dispersive excitations in the mid-infrared region (MIR, 100-500 meV), as well as $d-d$ ($E > 1.3$ eV,⁴²) excitations. To illustrate the relation between EI-RXS and RIXS, we integrate the RIXS spectra over a large energy range, $(-0.06, 10)$ eV. The result is a single momentum distribution curve, Fig.1(c), that emulates previous EI-RXS measurements of NCCO¹⁴. Note that the CO peak constitutes only a small fraction of the integrated intensity ($\approx 1\%$, similar to actual EI-RXS measurements^{9,10,13,26,39}) and that the large background comes from all other elastic and inelastic scattering within the energy-integration range. Therefore, the peak at Q_{CO} in an EI-RXS experiment is not necessarily restricted to elastic contributions, and it may originate from excitations with energies anywhere within a window of several electron-volts. Our RIXS experiments aim to dissect the inelastic spectrum of NCCO near Q_{CO} .

Figure 2(a) shows the detailed structure of the excitations in the non-SC NCCO sample at 25 K. Following previous EI-RXS measurements, we maximize the sensitivity to the CO by setting the polarization of the incoming photons parallel to the CuO_2 planes (σ incoming polarization) in back scattering (using grazing incidence, $H < 0$ in our convention)⁴¹. With this geometry, broad

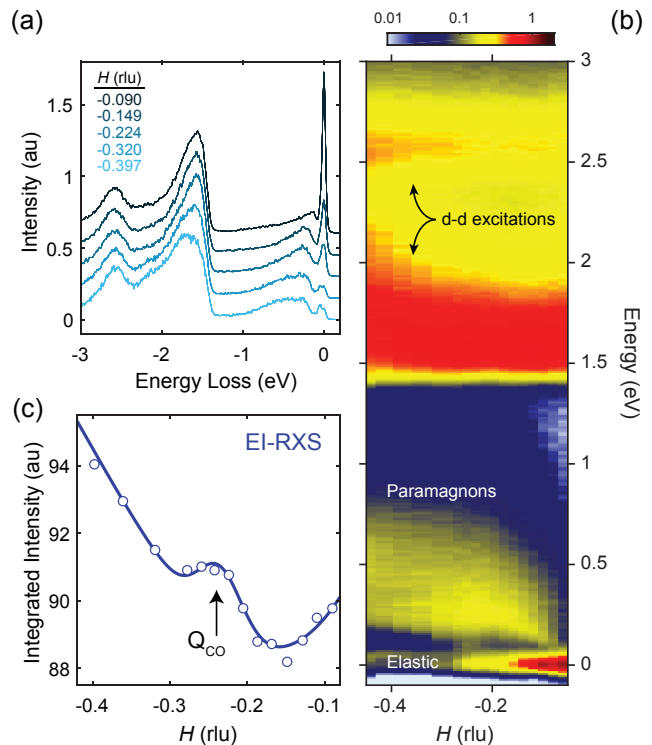


FIG. 1. (a), Cu- L_3 RIXS spectra for selected values of in-plane momentum transfer H . The curves are vertically offset for clarity. (b), Energy-momentum colormap of RIXS excitations. (c), EI-RXS momentum dependence obtained from the integrated RIXS spectra in the $(-0.06, 10)$ eV range. The measurements were performed on the non-SC sample, at 25 K, in σ scattering geometry. The color scale in (b) is logarithmic and in the same units as (a).

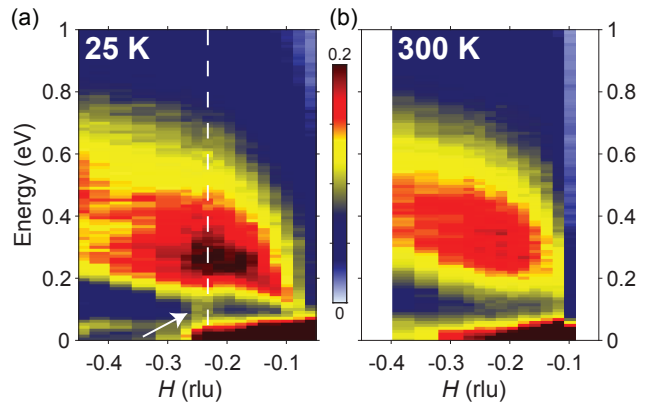


FIG. 2. Energy-momentum structure of the excitations in NCCO 0.106 measured with σ scattering at (a) 25 K and (b) 300 K. The dashed line in (a) marks Q_{CO} obtained from the energy-integrated data in Fig.1(c)⁴¹. The variable pixel size in (a)-(b) reflects the values of H and E for which the raw data was acquired.

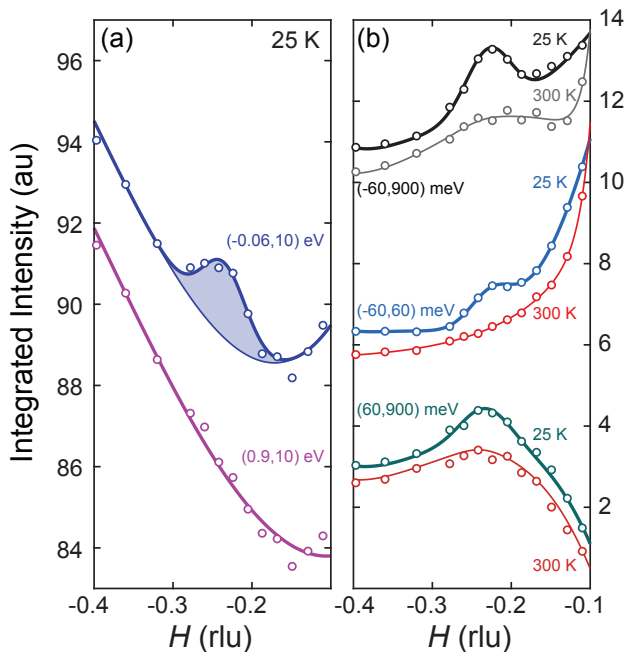


FIG. 3. (a), 25 K RIXS signal integrated over different energy ranges showing that the peak at Q_{CO} originates from energies below 900 meV. (b), Energy-integrated RIXS for 25 K and 300 K in the energy ranges marked on the figure. The line for the (0.9, 10) eV data in (a) and the line for (-60, 60) meV 300 K data in (b) are polynomial fits to the data. All the other lines represent a fit to the data using a polynomial for the background plus a Gaussian function for the peak. The data are vertically offset for clarity. All data on the non-SC sample in σ -geometry.

dispersive modes in the MIR and below include contributions from charge, spin, and phonon excitations^{43–49}. In particular, single spin-flip excitations in doped cuprates, have been named paramagnons, as they are the analogue to the magnon excitations in the AF undoped compound. Paramagnons have been detected in a variety of RIXS measurements and appear as damped but well-defined dispersive modes in the MIR region of the spectrum^{44–46,50,51}. For NCCO, MIR charge modes that exist only near the zone center ($|H| < 0.1$ rlu) have also been reported^{46,51} but they are outside the scope of our study. We note that our measurements show an excellent agreement with the paramagnon dispersion obtained from previous RIXS measurements^{41,46}. In our measurements, we find clear signals at Q_{CO} near the paramagnon energies. This is manifest in the raw data as a dynamic signal at Q_{CO} below the paramagnon energies and above the quasielastic line, marked by the white arrow in Fig. 2(a) ($E \approx 100$ meV), accompanied by a scattering enhancement at higher energies ($E \approx 250$ meV). Comparing this low-temperature measurement to its counterpart at 300 K, Fig. 2(b), we find that these two features are mostly suppressed, in agreement with the temperature dependence of the CO obtained from the EI-RXS measurements¹⁴. Similar features are observed at Q_{CO} in

all possible scattering geometries (positive and negative H , and σ/π scattering; see Fig. 2 and⁴¹), and on the SC NCCO sample near optimal doping ($T_c = 19$ K)⁴¹ following the previously established doping dependence of Q_{CO} ^{14,41}.

Not immediately clear from the data in Fig. 2(a) is the presence of a CO peak in the quasi-elastic line. In order to clearly establish its presence and to quantify its strength relative to the inelastic signal at Q_{CO} , we separate the RIXS excitation spectrum into different energy regions by constructing energy-integrated momentum distribution curves. First, Fig. 3(a) shows a comparison of the signal integrated over all measurable energies, (-0.06, 10) eV range, to the curve obtained by integrating over the (0.9, 10) eV range, which indicates that the peak at Q_{CO} is fully contained below 0.9 eV. Keeping in mind the energy resolution of these measurements ($\Delta E \approx 60$ meV), in Fig. 3(b) we decompose the Q_{CO} signal into quasi-elastic, (-60, 60) meV, and inelastic, (60, 900) meV, contributions. Comparing the the low and high temperature data, this analysis shows that roughly half of the peak observed in the EI-RXS measurements at low temperatures comes from inelastic scattering. The decomposition in Fig. 3(b) also shows that although suppressed, the short-range correlations at Q_{CO} are still present at 300 K, in agreement with previous EI-RXS measurements¹⁴. However, while at room temperature the quasi-elastic component at Q_{CO} is completely absent, a small inelastic contribution remains in the (60, 900) meV range. We further note that at 300 K there are no CO correlations in the (-60, 150) meV range,⁴¹. This indicates that any temperature dependence below 150 meV is strictly due to electronic degrees of freedom since all significant known phonon modes lie below that energy⁵².

Now focusing on the MIR enhancement, it is imperative to determine whether it is purely due to charge scattering that coexists with the magnetic excitations, or whether it arises from additional spin-flip scattering at Q_{CO} . To investigate this issue, we first acquired Cu- L_3 RIXS spectra with highest resolution currently possible ($\Delta E \approx 35$ meV), on and off Q_{CO} , Fig. 4(a), which clearly corroborate the observation that the MIR CO signal exists at the same energy as the paramagnons. Although intriguing, this observation alone does not demonstrate the magnetic nature of the dynamic correlations at Q_{CO} . However, with the ability to resolve $\sigma\pi'$ scattering, where the prime is added to represent the polarization of the scattered photons, it is possible to isolate single spin-flip excitations. Fortunately, a newly developed polarimeter (based on the concept described in Ref. ⁵³) allowed us to perform such measurements, albeit with the compromise of a lower energy resolution ($\Delta E \approx 90$ meV). Figure 4(b) shows the RIXS $\sigma\pi'$ cross-section, which primarily follows the paramagnon dispersion, as expected for spin-flip scattering. Remarkably, the intensity of the paramagnons shows a measurable enhancement exactly at Q_{CO} , while no vestige of the dynamic signal was de-

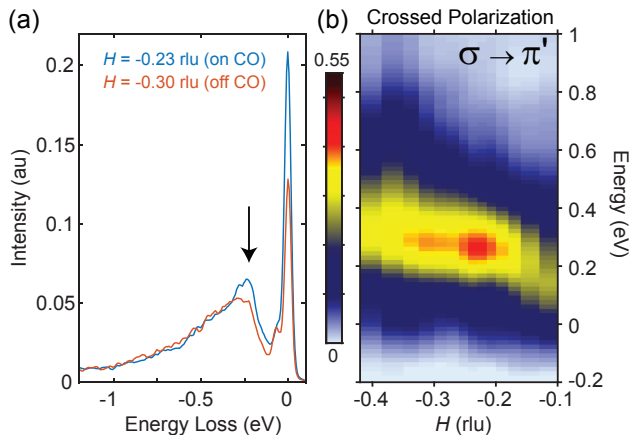


FIG. 4. (a) 25 K high energy-resolution (35 meV) spectra taken on the non-SC NCCO, with incoming σ polarization, for two H values, on and off Q_{CO} . (b) Energy-momentum structure for the excitations in the non-SC NCCO in the $\sigma\pi'$ channel, which is primarily composed of single spin-flip processes. The color plot in (b) was generated from eight polarization-resolved spectra⁴¹.

tected in the $\sigma\sigma'$ channel⁴¹.

Having established the magnetic nature of the dynamic correlations at Q_{CO} , it is important to discuss its relationship to the charge degrees of freedom. We first note that we do not resolve a peak at Q_{CO} in the quasielastic $\sigma\pi'$ channel, Fig. 4(b). It then follows that the quasielastic peak at Q_{CO} , see Fig. 3(b), must originate from charge correlations. Therefore, it is possible that two related effects occur at low temperatures: (i) a softening of the electronic response below 150 meV that results in static charge order, (ii) concomitant with a magnetic spectral weight enhancement at higher energies, centered at 250 meV. The observation that the majority of the dynamic response at Q_{CO} requires a flip of the electronic spin, does not rule out the presence of dynamic charge correlations at energies lower than that of the paramagnons, as predicted in Ref. ⁵⁴. Indeed, since that low-energy signal is weaker than the MIR enhancement, Fig. 2(a), its detection in the $\sigma\sigma'$ channel may still be beyond the sensitivity of the current state-of-the-art polarimetric RIXS instrumentation. Below, we provide an explanation for how fluctuations of the charge order pattern may result in (ii), whereas in regards to (i), we note that the softening of the charge susceptibility at Q_{CO} is predicted for CO with a d -wave symmetry in electron-doped cuprates^{54,55}.

To reconcile the presence of charge order and dynamic spin-flip correlations, first note that the fluctuations of a CO pattern will necessarily require a transfer of charge between neighboring sites, regardless of the mode of fluctuation – phase shifts or amplitude enhancements. In fact, to conform to the underlying antiferromagnetic correlations, which are strong in electron-doped cuprates, such CO-related inter-site processes must in-

volve a change of the spin degree of freedom. Since in this scenario a fluctuation of the charge-order pattern is coupled to a spin-flip process, it naturally follows that its excitation energy will largely be determined by the paramagnon energy scale at Q_{CO} . Nevertheless, lower-energy charge excitations near Q_{CO} should remain possible since doping weakens the underlying antiferromagnetic correlations in NCCO. Still, our measurements indicate that a majority of the dynamic correlations at Q_{CO} are magnetic in nature.

Despite the high Cu- L_3 RIXS energy-resolution of our measurements, we are not able to exclude the possibility that the quasi-elastic signal at Q_{CO} is (i) purely dynamic and/or (ii) purely magnetic. Regarding (i), we make a comparison to the hole-doped system $\text{Bi}_2\text{Sr}_{2-x}\text{La}_x\text{CuO}_{6+\delta}$, where the CO peaks measured by EI-RXS are very similar to the ones in NCCO in intensity, width and wave vector⁹. Additionally, a similar dynamic enhancement has also been observed in Cu- L_3 RIXS measurements of $\text{Bi}_2\text{Sr}_{2-x}\text{La}_x\text{CuO}_{6+\delta}$ ⁴⁷, although without polarization resolution. However, in $\text{Bi}_2\text{Sr}_{2-x}\text{La}_x\text{CuO}_{6+\delta}$, scanning tunneling spectroscopy (STS) measurements confirm a static charge order at the wave vector indicated by EI-RXS⁹. Completing the parallel between the two systems, we conclude that probes of charge correlations at long time scales, such as STS, would be able to confirm the existence of static charge order in NCCO at low temperatures. And regarding (ii), we note that we do not observe a peak at Q_{CO} in the quasielastic $\sigma\pi'$ channel and that there are no reports of magnetic order at Q_{CO} from spin-sensitive scattering probes such as neutron scattering.

Overall, our results provide support for the link between charge order and magnetic fluctuations that is present in many theoretical works of the cuprates^{21–24}. The data presented here is also consistent with a recent theoretical prediction⁵⁴, which indicates that the observed softening of the electronic response may be the first signature that the charge order in NCCO has a d -wave form factor, akin to the observations in $\text{YBa}_2\text{Cu}_3\text{O}_{6+\delta}$ and $\text{Bi}_2\text{Sr}_2\text{CaCu}_2\text{O}_{8+\delta}$,^{56–58}. This not only expands the similarities between charge order in hole and electron doped systems, it may also have implications for the mechanism of superconductivity in the electron-doped cuprates: a quantum Monte Carlo study showed that a d -wave CO at the measured Q_{CO} implies the presence of nematic fluctuations that also enhance d -wave superconductivity⁵⁹. Finally, our systematic investigations provide a precedent for similar investigations in other hole- and electron-doped cuprates. Depending on the strength of the effect, a similar coupling might be detectable in those materials by future RIXS studies following the methodology described here.

ACKNOWLEDGMENTS

We thank the ESRF for the allocation of synchrotron radiation beamtime. We acknowledge G. Ghiringhelli, L. Braicovich, R. Fumagalli and E. Weschke for fruitful discussions. This research was undertaken thanks in part to funding from the Max Planck-UBC-UTokyo Centre for Quantum Materials and the Canada First Research Excellence Fund, Quantum Materials and Future Technologies Program. The work at UBC was supported by the

Killam, Alfred P. Sloan, and Natural Sciences and Engineering Research Council of Canada's (NSERC's) Steacie Memorial Fellowships (A.D.); the Alexander von Humboldt Fellowship (A.D.); the Canada Research Chairs Program (A.D.); and the NSERC, Canada Foundation for Innovation (CFI), and CIFAR Quantum Materials. The work at the University of Minnesota was supported by the NSF through the University of Minnesota Materials Research Science and Engineering Center under award no. DMR-1420013.

- * ehda@ucdavis.edu
 † damascelli@physics.ubc.ca
- ¹ J. M. Tranquada, B. J. Sternlieb, J. D. Axe, Y. Nakamura, and S. Uchida, *Nature* **375**, 561 (1995).
 - ² J. E. Hoffman, E. W. Hudson, K. M. Lang, V. Madhavan, H. Eisaki, S. Uchida, and J. C. Davis, *Science* **295**, 466 (2002).
 - ³ C. Howald, H. Eisaki, N. Kaneko, and A. Kapitulnik, *Proceedings of the National Academy of Sciences* **100**, 9705 (2003).
 - ⁴ P. Abbamonte, A. Rusydi, S. Smadici, G. D. Gu, G. A. Sawatzky, and D. L. Feng, *Nature Physics* **1**, 155 (2005).
 - ⁵ T. Wu, H. Mayaffre, S. Kramer, M. Horvatic, C. Berthier, W. N. Hardy, R. Liang, D. A. Bonn, and M.-H. Julien, *Nature* **477**, 191 (2011).
 - ⁶ G. Ghiringhelli, M. Le Tacon, M. Minola, S. Blanco-Canosa, C. Mazzoli, N. B. Brookes, G. M. De Luca, A. Frano, D. G. Hawthorn, F. He, T. Loew, M. M. Sala, D. C. Peets, M. Salluzzo, E. Schierle, R. Sutarto, G. A. Sawatzky, E. Weschke, B. Keimer, and L. Braicovich, *Science* **337**, 821 (2012).
 - ⁷ J. Chang, E. Blackburn, A. T. Holmes, N. B. Christensen, J. Larsen, J. Mesot, R. Liang, D. A. Bonn, W. N. Hardy, A. Watenphul, M. v. Zimmermann, E. M. Forgan, and S. M. Hayden, *Nature Physics* **8**, 871 (2012).
 - ⁸ A. J. Achkar, R. Sutarto, X. Mao, F. He, A. Frano, S. Blanco-Canosa, M. Le Tacon, G. Ghiringhelli, L. Braicovich, M. Minola, M. Moretti Sala, C. Mazzoli, R. Liang, D. A. Bonn, W. N. Hardy, B. Keimer, G. A. Sawatzky, and D. G. Hawthorn, *Phys. Rev. Lett.* **109**, 167001 (2012).
 - ⁹ R. Comin, A. Frano, M. M. Yee, Y. Yoshida, H. Eisaki, E. Schierle, E. Weschke, R. Sutarto, F. He, A. Soumyanarayanan, Y. He, M. Le Tacon, I. S. Elfimov, J. E. Hoffman, G. A. Sawatzky, B. Keimer, and A. Damascelli, *Science* **343**, 390 (2014).
 - ¹⁰ E. H. da Silva Neto, P. Aynajian, A. Frano, R. Comin, E. Schierle, E. Weschke, A. Gyenis, J. Wen, J. Schneeloch, Z. Xu, S. Ono, G. Gu, M. Le Tacon, and A. Yazdani, *Science* **343**, 393 (2014).
 - ¹¹ M. Hashimoto, G. Ghiringhelli, W.-S. Lee, G. Dellea, A. Amorese, C. Mazzoli, K. Kummer, N. B. Brookes, B. Moritz, Y. Yoshida, H. Eisaki, Z. Hussain, T. P. Devereaux, Z.-X. Shen, and L. Braicovich, *Phys. Rev. B* **89**, 220511 (2014).
 - ¹² W. Tabis, Y. Li, M. Le Tacon, L. Braicovich, A. Kreyssig, M. Minola, G. Dellea, E. Weschke, M. J. Veit, M. Ramazanoglu, A. I. Goldman, T. Schmitt, G. Ghiringhelli, N. Barišić, M. K. Chan, C. J. Dorow, G. Yu, X. Zhao, B. Keimer, and M. Greven, *Nat. Comm.* **5** (2014).
 - ¹³ E. H. da Silva Neto, R. Comin, F. He, R. Sutarto, Y. Jiang, R. L. Greene, G. A. Sawatzky, and A. Damascelli, *Science* **347**, 282 (2015).
 - ¹⁴ E. H. da Silva Neto, B. Yu, M. Minola, R. Sutarto, E. Schierle, F. Boschini, M. Zonno, M. Bluschke, J. Higgins, Y. Li, G. Yu, E. Weschke, F. He, M. Le Tacon, R. L. Greene, M. Greven, G. A. Sawatzky, B. Keimer, and A. Damascelli, *Science Advances* **2**, e1600782 (2016).
 - ¹⁵ W. Tabis, B. Yu, I. Bialo, M. Bluschke, T. Kolodziej, A. Kozłowski, E. Blackburn, K. Sen, E. M. Forgan, M. v. Zimmermann, Y. Tang, E. Weschke, B. Vignolle, M. Heping, H. Gretarsson, R. Sutarto, F. He, M. Le Tacon, N. Barišić, G. Yu, and M. Greven, *Phys. Rev. B* **96**, 134510 (2017).
 - ¹⁶ H. Jang, S. Asano, M. Fujita, M. Hashimoto, D. H. Lu, C. A. Burns, C.-C. Kao, and J.-S. Lee, *Phys. Rev. X* **7**, 041066 (2017).
 - ¹⁷ J. Zaanen and O. Gunnarsson, *Phys. Rev. B* **40**, 7391 (1989).
 - ¹⁸ K. Machida, *Physica C: Superconductivity* **158**, 192 (1989).
 - ¹⁹ M. Kato, K. Machida, H. Nakanishi, and M. Fujita, *Journal of the Physical Society of Japan* **59**, 1047 (1990).
 - ²⁰ S. A. Kivelson, E. Fradkin, and V. J. Emery, *Nature* **393**, 550 (1998).
 - ²¹ J. C. S. Davis and D.-H. Lee, *Proceedings of the National Academy of Sciences* **110**, 17623 (2013).
 - ²² K. B. Efetov, H. Meier, and C. Pepin, *Nat Phys* **9**, 442 (2013).
 - ²³ S. Sachdev and R. La Placa, *Phys. Rev. Lett.* **111**, 027202 (2013).
 - ²⁴ Y. Wang and A. Chubukov, *Phys. Rev. B* **90**, 035149 (2014).
 - ²⁵ X. Wang, Y. Wang, Y. Schattner, E. Berg, and R. M. Fernandes, *Phys. Rev. Lett.* **120**, 247002 (2018).
 - ²⁶ S. Blanco-Canosa, A. Frano, E. Schierle, J. Porras, T. Loew, M. Minola, M. Bluschke, E. Weschke, B. Keimer, and M. Le Tacon, *Phys. Rev. B* **90**, 054513 (2014).
 - ²⁷ M. Hücker, N. B. Christensen, A. T. Holmes, E. Blackburn, E. M. Forgan, R. Liang, D. A. Bonn, W. N. Hardy, O. Gutowski, M. v. Zimmermann, S. M. Hayden, and J. Chang, *Phys. Rev. B* **90**, 054514 (2014).
 - ²⁸ S. Blanco-Canosa, A. Frano, T. Loew, Y. Lu, J. Porras, G. Ghiringhelli, M. Minola, C. Mazzoli, L. Braicovich, E. Schierle, E. Weschke, M. Le Tacon, and B. Keimer, *Phys. Rev. Lett.* **110**, 1 (2013).

- ²⁹ T. Wu, H. Mayaffre, S. Krämer, M. Horvatić, C. Berthier, W. N. Hardy, R. Liang, D. A. Bonn, and M.-H. Julien, *Nat Commun* **6** (2015).
- ³⁰ E. M. Motoyama, G. Yu, I. M. Vishik, O. P. Vajk, P. K. Mang, and M. Greven, *Nature* **445**, 186 (2007).
- ³¹ M. Le Tacon, A. Bosak, S. M. Souliou, G. Dellea, T. Loew, R. Heid, K.-P. Bohnen, G. Ghiringhelli, M. Krisch, and B. Keimer, *Nat Phys* **10**, 52 (2014).
- ³² S. Gerber, H. Jang, H. Nojiri, S. Matsuzawa, H. Yasumura, D. A. Bonn, R. Liang, W. N. Hardy, Z. Islam, A. Mehta, S. Song, M. Sikorski, D. Stefanescu, Y. Feng, S. A. Kivelson, T. P. Devereaux, Z.-X. Shen, C.-C. Kao, W.-S. Lee, D. Zhu, and J.-S. Lee, *Science* **350**, 949 (2015).
- ³³ J. Chang, E. Blackburn, O. Ivashko, A. T. Holmes, N. B. Christensen, M. Hcker, R. Liang, D. A. Bonn, W. N. Hardy, U. Rtt, M. v. Zimmermann, E. M. Forgan, and S. M. Hayden, *Nature Communications* **7**, 11494 (2016).
- ³⁴ H. Jang, W.-S. Lee, H. Nojiri, S. Matsuzawa, H. Yasumura, L. Nie, A. V. Maharaj, S. Gerber, Y.-J. Liu, A. Mehta, D. A. Bonn, R. Liang, W. N. Hardy, C. A. Burns, Z. Islam, S. Song, J. Hastings, T. P. Devereaux, Z.-X. Shen, S. A. Kivelson, C.-C. Kao, D. Zhu, and J.-S. Lee, *Proceedings of the National Academy of Sciences* **113**, 14645 (2016).
- ³⁵ S. A. Kivelson, I. P. Bindloss, E. Fradkin, V. Oganessian, J. M. Tranquada, A. Kapitulnik, and C. Howald, *Rev. Mod. Phys.* **75**, 1201 (2003).
- ³⁶ Y. Caplan, G. Wachtel, and D. Orgad, *Phys. Rev. B* **92**, 224504 (2015).
- ³⁷ T. Wu, R. Zhou, M. Hirata, I. Vinograd, H. Mayaffre, R. Liang, W. N. Hardy, D. A. Bonn, T. Loew, J. Porras, D. Haug, C. T. Lin, V. Hinkov, B. Keimer, and M.-H. Julien, *Phys. Rev. B* **93**, 134518 (2016).
- ³⁸ L. Chaix, G. Ghiringhelli, Y. Y. Peng, M. Hashimoto, B. Moritz, K. Kummer, N. B. Brookes, Y. He, S. Chen, S. Ishida, Y. Yoshida, H. Eisaki, M. Salluzzo, L. Braicovich, Z.-X. Shen, T. P. Devereaux, and W.-S. Lee, *Nature Physics* **13**, 952 (2017).
- ³⁹ V. Thampy, M. P. M. Dean, N. B. Christensen, L. Steinke, Z. Islam, M. Oda, M. Ido, N. Momono, S. B. Wilkins, and J. P. Hill, *Phys. Rev. B* **90**, 100510 (2014).
- ⁴⁰ P. K. Mang, S. Laroche, A. Mehta, O. P. Vajk, A. S. Erickson, L. Lu, W. J. L. Buyers, A. F. Marshall, K. Prokes, and M. Greven, *Phys. Rev. B* **70**, 094507 (2004).
- ⁴¹ See supplemental materials.
- ⁴² M. M. Sala, V. Bisogni, C. Aruta, G. Balestrino, H. Berger, N. B. Brookes, G. M. de Luca, D. D. Castro, M. Grioni, M. Guarise, P. G. Medaglia, F. M. Granozio, M. Minola, P. Perna, M. Radovic, M. Salluzzo, T. Schmitt, K. J. Zhou, L. Braicovich, and G. Ghiringhelli, *New Journal of Physics* **13**, 043026 (2011).
- ⁴³ L. J. P. Ament, M. van Veenendaal, T. P. Devereaux, J. P. Hill, and J. van den Brink, *Rev. Mod. Phys.* **83**, 705 (2011).
- ⁴⁴ L. Braicovich, J. van den Brink, V. Bisogni, M. M. Sala, L. J. P. Ament, N. B. Brookes, G. M. De Luca, M. Salluzzo, T. Schmitt, V. N. Strocov, and G. Ghiringhelli, *Phys. Rev. Lett.* **104**, 077002 (2010).
- ⁴⁵ M. Le Tacon, G. Ghiringhelli, J. Chaloupka, M. M. Sala, V. Hinkov, M. W. Haverkort, M. Minola, M. Bakr, K. J. Zhou, S. Blanco-Canosa, C. Monney, Y. T. Song, G. L. Sun, C. T. Lin, G. M. De Luca, M. Salluzzo, G. Khaliullin, T. Schmitt, L. Braicovich, and B. Keimer, *Nat. Phys.* **7**, 725 (2011).
- ⁴⁶ W. S. Lee, J. J. Lee, E. A. Nowadnick, S. Gerber, W. Tabis, S. W. Huang, V. N. Strocov, E. M. Motoyama, G. Yu, B. Moritz, H. Y. Huang, R. P. Wang, Y. B. Huang, W. B. Wu, C. T. Chen, D. J. Huang, M. Greven, T. Schmitt, Z. X. Shen, and T. P. Devereaux, *Nat Phys* **10**, 883 (2014).
- ⁴⁷ Y. Y. Peng, M. Hashimoto, M. M. Sala, A. Amorese, N. B. Brookes, G. Dellea, W.-S. Lee, M. Minola, T. Schmitt, Y. Yoshida, K.-J. Zhou, H. Eisaki, T. P. Devereaux, Z.-X. Shen, L. Braicovich, and G. Ghiringhelli, *Phys. Rev. B* **92**, 064517 (2015).
- ⁴⁸ C. Jia, K. Wohlfeld, Y. Wang, B. Moritz, and T. P. Devereaux, *Phys. Rev. X* **6**, 021020 (2016).
- ⁴⁹ T. P. Devereaux, A. M. Shvaika, K. Wu, K. Wohlfeld, C. J. Jia, Y. Wang, B. Moritz, L. Chaix, W.-S. Lee, Z.-X. Shen, G. Ghiringhelli, and L. Braicovich, *Phys. Rev. X* **6**, 041019 (2016).
- ⁵⁰ J. P. Hill, G. Blumberg, Y.-J. Kim, D. S. Ellis, S. Wakimoto, R. J. Birgeneau, S. Komiyama, Y. Ando, B. Liang, R. L. Greene, D. Casa, and T. Gog, *Phys. Rev. Lett.* **100**, 097001 (2008).
- ⁵¹ K. Ishii, M. Fujita, T. Sasaki, M. Minola, G. Dellea, C. Mazzoli, K. Kummer, G. Ghiringhelli, L. Braicovich, T. Tohyama, K. Tsutsumi, K. Sato, R. Kajimoto, K. Ikeuchi, K. Yamada, M. Yoshida, M. Kurooka, and J. Mizuki, *Nature Communications* **5**, 3714 (2014).
- ⁵² M. d'Astuto, P. K. Mang, P. Giura, A. Shukla, P. Ghigna, A. Mirone, M. Braden, M. Greven, M. Krisch, and F. Sette, *Phys. Rev. Lett.* **88**, 167002 (2002).
- ⁵³ L. Braicovich, M. Minola, G. Dellea, M. L. Tacon, M. M. Sala, C. Morawe, J.-C. Peffen, R. Supruangnet, F. Yakhov, G. Ghiringhelli, and N. B. Brookes, *Review of Scientific Instruments* **85**, 115104 (2014).
- ⁵⁴ M. Bejas, H. Yamase, and A. Greco, *Phys. Rev. B* **96**, 214513 (2017).
- ⁵⁵ H. Yamase, M. Bejas, and A. Greco, *ArXiv* (2018), 1808.03618.
- ⁵⁶ R. Comin, R. Sutarto, F. He, E. H. da Silva Neto, L. Chauviere, A. Frano, R. Liang, W. N. Hardy, D. A. Bonn, Y. Yoshida, H. Eisaki, A. J. Achkar, D. G. Hawthorn, B. Keimer, G. A. Sawatzky, and A. Damascelli, *Nat. Mat.* **14**, 796 (2015).
- ⁵⁷ K. Fujita, M. H. Hamidian, S. D. Edkins, C. K. Kim, Y. Kohsaka, M. Azuma, M. Takano, H. Takagi, H. Eisaki, S.-i. Uchida, A. Allais, M. J. Lawler, E.-A. Kim, S. Sachdev, and J. C. S. Davis, *Proc. Natl. Acad. Sci. (PNAS)* **111**, E3026 (2014).
- ⁵⁸ A. J. Achkar, F. He, R. Sutarto, C. McMahon, M. Zwiebler, M. Hcker, G. D. Gu, R. Liang, D. A. Bonn, W. N. Hardy, J. Geck, and D. G. Hawthorn, *Nat. Mat.* **15**, 616 (2016).
- ⁵⁹ Z.-X. Li, F. Wang, H. Yao, and D.-H. Lee, *Phys. Rev. B* **95**, 214505 (2017).